Construction and Building Materials 451 (2024) 138849

Contents lists available at ScienceDirect

Construction and Building Materials

journal homepage: www.elsevier.com/locate/conbuildmat

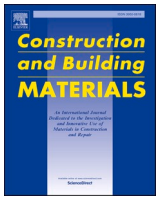

Engineered cementitious composite with nanocellulose and high-volume fly ash

H. Withana [a], S. Rawat [a], Daniel.J. Fanna [b], Y.X. Zhang [a,*]

[a] School of Engineering, Design and Built Environment, Western Sydney University, NSW 2751, Australia
[b] Advanced Materials Characterisation Facility, Western Sydney University, NSW 2116, Australia

ARTICLE INFO

Keywords:
Engineered cementitious composite (ECC)
Green construction material
High-volume fly ash (HVFA)
Hybrid fibre
Nanocellulose (NC)

ABSTRACT

This research develops a sustainable Engineered Cementitious Composites (ECC) with reduced cement usage by incorporating high volume fly ash (HVFA) and silica fume, along with the novel application of nanocellulose (NC)- a plant-based nanomaterial- and hybrid fibres to achieve high strength and ductility simultaneously. 12 mixes were developed including three base ECC mixes with 1.5 % polyethylene (PE) and 0.5 % steel fibres with varying proportions of fly ash and silica fume (1.2:0–1:0.2) and nine NC reinforced ECC mixes with varying dosages of NC (0.15 %, 0.2 %, 0.25 % by weight). The effect of fly ash/silica fume ratio and NC on mechanical properties was investigated through compressive and uniaxial tensile tests. Scanning electron microscope (SEM) and differential scanning calorimetry (DSC) techniques were utilized to gain insights into the HVFA and NC matrix systems as well as the mechanisms of NC and hybrid fibres. Results showed that reducing the fly ash/silica fume ratio increased strength but reduced tensile strain. Incorporating NC improved strength across all mixes, irrespective of fly ash/silica fume content, with the mix containing 0.2 % NC showing the highest improvement. This novel ECC is anticipated to offer a sustainable and high-performance material solution for engineering structures.

1. Introduction

The brittle nature of concrete and the environmental impact of concrete manufacturing due to extensive cement use demand more ductile and sustainable material solution for construction. Engineered cementitious composites (ECCs), a unique class of high-performance fibre reinforced cementitious composites with significant strain hardening behaviour, were developed to address the issue of material brittleness [1]. Mono fibre ECCs were first evolved with a single fibre reinforcement using either a high modulus fibre such as steel or a relatively low modulus fibre such as polyethylene (PE). This was later expanded to hybrid ECCs where, by employing appropriate volumes of both high and low modulus fibres in combination, improvements in both high strength and high strain capabilities were achieved [2–5]. However, achieving considerable strength improvements with ECC requires the use of high amounts of cement [6], which undermines the sustainability of the ECCs, as cement production emits 8 % of global CO_2 [7].

To address the sustainability issue of ECCs, new forms of ECCs have been developed, replacing large amounts of cement with industry by-products such as fly ash. The term “high volume fly ash (HVFA)” concrete refers to a concrete material with more fly ash than cement, typically around 50–60 % fly ash by mass of total cementitious material [6]. Research indicates that although substituting cement with a substantial amount of fly ash enhances sustainability, it results in a decrease in both compressive and flexural strengths [6]. The spherical shape of the particles of fly ash elevates porosity of the composite, lowering the matrix interface bond and the matrix densification [8]. Therefore, the ECCs developed by replacing cement with high volumes of fly ash often have notably lower strengths [9]. To address these issues, supplementary cementitious materials such as ground granulated blast furnace slag [10], blends of silica fume and fly ash with fly ash cenosphere as filler [11], and rice husk ash [12] have been successfully used. Additionally, in recent years, nanomaterials have gained significant research interest as supplementary reinforcing materials in cementitious composites due to their unique size and properties [13].

A wide range of studies have documented significant improvements in the mechanical properties of cementitious materials by using nanomaterials, specifically compressive and flexural strength [14–16]. Nanomaterials are distributed at a finer scale, with close spacing of individual nano reinforcements with each other [16,17]. They possess a

* Corresponding author.
E-mail address: sarah.zhang@westernsydney.edu.au (Y.X. Zhang).

https://doi.org/10.1016/j.conbuildmat.2024.138849
Received 6 April 2024; Received in revised form 12 October 2024; Accepted 18 October 2024
Available online 21 October 2024

larger surface area relative to their volume, which enhances interactions between fibre and matrix allowing better bonding and stress distribution across the matrix [18,19]. On the contrary, the fibres employed in ECCs have relatively smaller surface areas, limiting the interfacial strength by entrapping air voids and reducing their contribution to strength improvements. When nanomaterials are added to the cement matrix, they act as a filling agent, hindering the formation of micro-sized pores or gaps and densifying the matrix. Therefore, it is reasonable to assume that nanomaterial reinforcement, which provides modifications at the nanoscale, could be an effective approach to counteract the strength loss resulting from the inclusion of HVFA in ECCs, while maintaining the ductility achieved through the use of hybrid fibres.

However, difficulties in fine dispersion in matrix and high production costs limits the widespread application of nanomaterials [17,20]. Due to the large surface area and high aspect ratio of nanomaterials, the presence of Van der Waals forces often leads to the formation of clumps, resulting in voids within the matrix, and consequently, impeding the mechanical properties of the composites [17]. Nanocellulose (NC), a plant-based nanomaterial, is a recent innovation in the field of nanomaterials. NC is a form of nanofibre that is derived from cellulose, which is the primary substance found in plant cell walls. Being an abundant natural ingredient, it is regarded as one of the most sustainable raw materials [21] with a cost-effective production process [22]. As lower concentrations of NC is usually needed, it is more feasible to achieve fine dispersion, and thus the prevalent challenge of nanomaterial agglomeration can be minimised by employing NC. Existing literatures utilizing NC in cementitious composites have reported remarkable improvements in strength with use of much lower dosages of NC, compared to conventional nano particles such as nanosilica. For instance, 26 % improvement of compressive strength was achieved with NC concentrations as low as 0.05 % by weight (wt.) [23], whereas 3 % (by wt.) of nanosilica was needed to improve the compressive strength by 24 % [24]. Moreover, NC has outstanding physical benefits and mechanical properties such as high modulus and strength, high aspect ratio and hydrophilic and hygroscopic properties, all of which are favourable to cement-fibre reinforcement system [25].

Although improvement of mechanical characteristics in nanocellulose-based composites has been established in the literatures, research into their use in cement-based composites, notably in ECC, has been minimal, and no research has been reported on using NC to reinforce hybrid fibre ECC so far. This study develops a novel hybrid PE-steel fibre reinforced ECC by incorporating HVFA and NC, aiming for simultaneous enhancement in sustainability and mechanical performance characterized by both high strength and ductility. Typically, high stiffness fibres provide high ultimate strength but have low strain capacity and small crack widths, while low stiffness fibres offer the opposite—lower ultimate strength, higher strain capacity, and larger crack widths [5]. Therefore, with hybrid application of both low modulus PE fibre and high modulus steel fibre, the ECC is expected to achieve an optimal balance between the strength and the ultimate strain capacity, as demonstrated in previous research studies [5,9,26]. To lower the carbon footprint, more than 50 % cement is replaced with fly ash. NC is employed to improve the denseness of the matrix, counteracting any potential reduction caused by the addition of HVFA, thereby improving the overall strength of the composite. Additionally, accompanying fly ash with silica fume has been reported in achieving a better balance between strength and strain [4]. Therefore, in this study, fly ash is combined with varying doses of silica fume to further optimize the mechanical performance. Microstructural characterization techniques such as scanning electron microscopy (SEM), and differential scanning calorimetry (DSC) analysis are further utilized to insightfully understand the behaviour of the HVFA matrix system and the mechanism for the effect of using NC and hybrid fibres.

2. Experimental programs

2.1. Materials

The raw materials used included cement, sand, water, fly ash, silica fume, high range water reducer (HRWR), steel fibres, PE fibres, and NC. General purpose ordinary Portland cement, class F fly ash and high-grade silica fume were used as the binding material, while sand of mean grain size 225 μm was used as fine aggregate. PE and steel fibres (Fig. 1a and b) were used as low modulus and high modulus fibres, respectively and their properties are detailed in Table 1. The cellulose nanofibrils (CNF) from Cellulose Lab, Canada was used as the NC. It was derived from bleached softwood pulp and prepared by subjecting to intensive mechanical treatment by a high-pressure homogenizer. CNF are micrometre long, flexible, and entangled fibrils made of bundles of stretched cellulose chain molecules. This type of NC is chosen in this study because they have a higher aspect ratio (length 500–2000 nm and diameter 1–100 nm) and a higher surface area due to their longer length as compared to the most common type of NC, cellulose nano whiskers (CNW). CNW have a lower aspect ratio (length 50–500 nm and diameter 2–20 nm), lower moduli (50–100 GPa) and limited flexibility due to the absence of amorphous portions, compared to CNF [27]. Unlike CNW, CNF exhibits both amorphous and crystalline parts and presents a web-like structure, which together with the higher aspect ratio is more favourable for creating ductile materials. It was received as a slurry in aqueous gel form (Fig. 1c) with 3.0 % by weight. The material properties of the NC is shown in Table 2. Additionally, polycarboxylate-based HRWR Rheobuild 10000N7 was used to attain sufficient workability for uniform fibre dispersion.

2.2. New mix designs of hybrid fibre ECC and NC reinforced ECC materials

Firstly, three base mix designs of hybrid ECCs with PE and steel fibres without NC were developed with varying combinations of silica fume and fly ash while keeping the cement/binder ratio at 45 % (i.e. less than 50 %). ECC-M45 mix [1] was used as a reference point for selecting the ingredients and weight proportions of the mixes. A fibre volume fraction of 2 % was adopted with 1.5 % PE fibre and 0.5 % steel fibre as this combination of fibres has exhibited an optimum balance of tensile strain and strength [28]. The purpose was to examine how the proportions of fly ash and silica fume influence the compressive and tensile properties, as well as Young's modulus, and identify the most optimal combination of fly ash and silica fume ratios.

In all the mixes, cement, fly ash/silica fume ratio was kept as 1:1.2 ensuring more than 50 % of cement replacement. Silica fume and fly ash levels were varied such that when the fly ash content was decreased by 0.1, the silica fume content was increased by the same amount while keeping the total silica fume + fly ash content constant. This approach was taken with the view of achieving an optimum balance between the material's compressive strength and ultimate tensile strain while also promoting greener construction practices. The water/binder ratio and sand/binder ratio were kept constant as 0.26 and 0.36 respectively as recommended by [3]. The mix ratios of the three mixes (denoted as MIX1, MIX2 and MIX3) are given in Table 3.

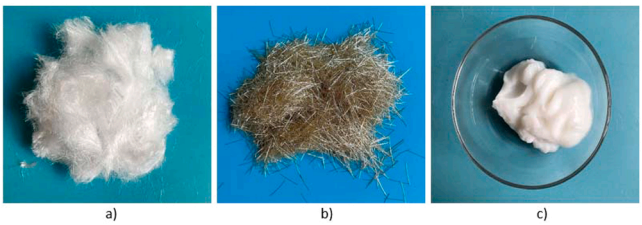

Fig. 1. Fibres used in this study: a) PE fibres; b) Steel fibres; c) NC (CNF).

Table 1
Properties of micro fibres.

Fibre type	Diameter (μm)	Length (mm)	Young's Modulus (GPa)	Tensile Strength (MPa)	Density (g/cm^3)	Aspect Ratio	Shape
PE	24	12	116	3000	0.97	500	Straight
Steel	200±3	13±1	200	2500	7.8	80	Straight

Table 2
Dimensions and mechanical properties of the NC (CNF).

Type of NC	CNF-Slurry-SMC (Unmodified)
Morphology	Aqueous gel slurry−1–3 % solids in water
Fibre Diameter	30–80 nm
Fibre Length	Up to several hundred microns
Fibre Density	1.0 g/cm^3
Surface group	Hydroxyl hydrophilic

After assessing the mechanical performance of these base mixes, PE-Steel ECC mixes were subsequently modified by incorporating NC, with the objective of further enhancing the material's strength. Nine more PE-Steel-NC mixes were developed by adding 0.15 %, 0.2 %, 0.25 % of NC (by weight) dosages to each base mix to study the effect of NC dosages. These dosages of NC were chosen based on a previous study by the authors, where the optimum dosage of NC that corresponds to the maximum strength was shown to be approximately 0.2 % [29]. The mix ratios of the nine mixes of ECCs with NC (NC-ECC) are given in Table 4.

2.3. Specimen casting

The mixing was prepared following the procedures mentioned in Rawat et al. [10] and Khan et al. [30]. Initially, the dry ingredients including cement, fly ash, silica fume and sand were mixed for about 2 minutes. Following this, water and HRWR were combined and gradually added to the dry mix while the mixing continued. Once the mix attained a homogenous state, the fibres were slowly added, and the mixing was continued for a few more minutes until all the fibres were evenly distributed. For mixes containing NC, the NC was mixed with water and dispersed evenly using a hand blender. Once a homogeneous dispersion without any clumps was ensured, the solution was added to fibre-cement mix and the mixing was continued for further 2–3 minutes. After achieving a uniform consistency, it was poured into moulds and vibrated for 30 seconds. Following this, the moulds were cling-wrapped and kept at room temperature for 24 hrs until demoulding. After demoulding, the specimens were wrapped in plastic sheets and placed in an environmental chamber maintained at a temperature of 23 ±1 ^{0}C and a relative humidity of 95 ± 5 % until the age of testing.

2.4. Testing procedures

Initially, a series of tests including compression, Young's modulus, and uniaxial tensile tests were conducted on the three base mixes of the PE-Steel ECCs. Thereafter, a series of compressive and tensile tests were carried out on the nine NC-ECC mixes, to investigate the effect of NC on compressive and tensile properties. The PE-Steel ECCs with no NC were used as a reference. SEM and DSC were further performed to study the microstructure of the developed mixes.

2.4.1. Compressive strength and Young's modulus

Instron universal testing machine of 1000 kN capacity was used to conduct the compression tests and Young's modulus tests in accordance with the Australian Standard AS 1012 [31]. Compressive test was conducted on 50 mm cubes at a loading rate of 20 MPa/min, while 100 mm diameter × 200 mm height cylinders were used to perform Young's modulus test. The Young's modulus was calculated by the taking the secant modulus at 40 % of the expected compressive strength. Three specimens were tested for each mix at 28 day curing age.

2.4.2. Uniaxial tensile test

Dog-bone specimens with a cross-sectional area of 30 mm × 13 mm in the reduced section and a gauge length of 80 mm (shown in Fig. 2a.) were used for the uniaxial tension test. The test method applied in this research was based on a previous study [32].

An Instron load frame with a 250 kN capacity with fixed hydraulic grips was used for testing. All the tests were conducted under displacement control at a loading rate of 0.5 mm/min. Two external

Table 3
Mix design for PE-Steel ECC (base) mixes.

Mix ID	Cement	Fly ash	Silica fume	Sand	Water	HRWR	Steel (%)	PE (%)
MIX1	1	1.2	0	0.8	0.57	0.012–0.02	0.5	1.5
MIX2	1	1.1	0.1					
MIX3	1	1	0.2					

Note: Fibre content is expressed in volume fraction of the mix, while all other ingredients are expressed as weight proportions relative to the cement content.

Table 4
Mix design for NC-ECC mixes.

Mix ID	Cement	Fly ash	Silica fume	Sand	Water	HRWR	Steel (%)	PE (%)	NC (%)
MIX1–0.15NC	1	1.2	0	0.8	0.57	0.012–0.02	0.5	1.5	0.15
MIX1–0.2NC									0.2
MIX1–0.25NC									0.25
MIX2–0.15NC	1	1.1	0.1						0.15
MIX2–0.2NC									0.2
MIX2–0.25NC									0.25
MIX3–0.15NC	1	1	0.2						0.15
MIX3–0.2NC									0.2
MIX3–0.25NC									0.25

Note: PE and steel fibre content are expressed in volume fraction and NC is expressed in weight fraction of the mix, while all other ingredients are expressed as weight proportions relative to the cement content.

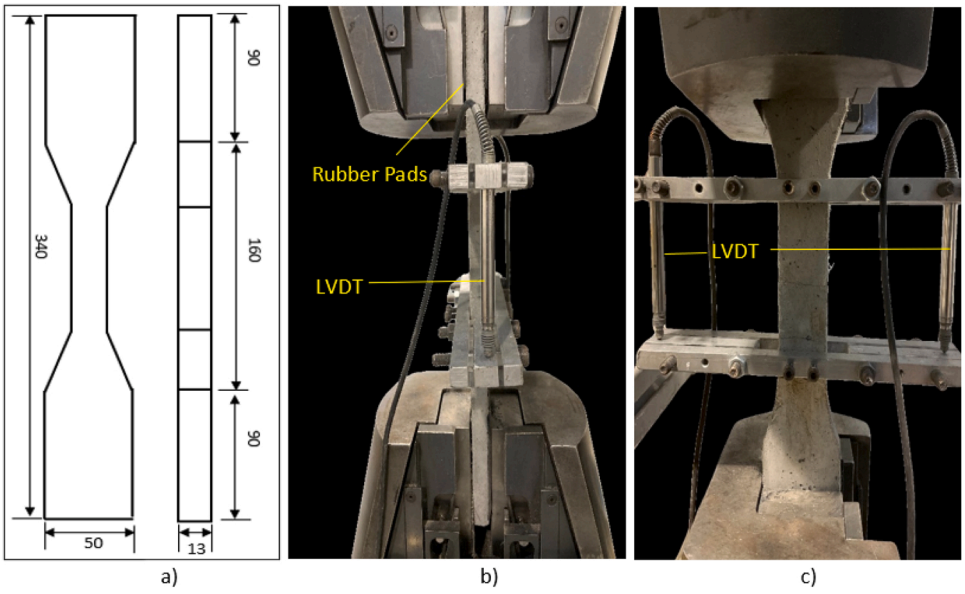

Fig. 2. Uniaxial tensile test: a) dog-bone specimen geometry (dimensions: mm); b) test set-up: side view; c) test set-up: front view.

linear variable displacement transducers (LVDT) were attached on either side of the specimen via a steel rig, to measure the displacement. Test setup for the uniaxial tensile test is shown in Fig. 2b and Fig. 2c. Six specimens were tested for each mix to obtain the static tensile stress-strain behaviour. However, due to random distribution of fibres, not all six specimens tested yielded consistent results. Therefore, the three most consistent results were chosen for analysis.

2.4.3. *Microstructural analysis*

The failure surface of the tested ECC was examined by using a high-resolution Zeiss field emission SEM and optical microscope. Small pieces from the fractured surface of the specimens were removed and prepared for the analysis by applying a gold coating for 60 seconds to mitigate the effect of surface charges induced by the ultrahigh-energy electron beam. A part of the same extracted sample was ground to pass through a 45 μm sieve, and the powdered sample was used for DSC analysis using Netzsch STA 449F3.

3. Effect of fly ash and silica fume on the mechanical properties

3.1. *Compressive properties*

The effect of fly ash/silica fume ratio on compressive strength and Young's modulus were examined by using the three base mixes of PE-Steel ECCs, i.e. MIX1, MIX2 and MIX3, with varying quantities of fly ash and silica fume. Fig. 3 shows the compressive strength of MIX1, MIX2 and MIX3 at 7-, 14- and 28-days curing age. The highest strength was observed in MIX3 while the lowest was seen in MIX1. It can be seen that as the fly ash content decreased and the silica fume content increased, the compressive strength increased at all ages. The 28-day strength was 51 %, 46 % and 41 % higher in MIX1, MIX2 and MIX3 respectively than their strength at 7 days.

The Young's modulus of the three mixes was obtained as 14.8 GPa, 18 GPa and 28 GPa for MIX1, MIX2 and MIX3 respectively, with the highest observed in MIX3 with the lowest fly ash content, and the lowest value for MIX1 which contained the highest fly ash content. All mixes exhibited a lower value of Young's modulus compared to conventional concrete (>30 GPa). As reported in the previous studies [3,30], this could be attributed to the absence of coarse aggregates in the ECC matrix. Since coarse aggregates are eliminated in the ECC matrix in order to enhance ductility, stiffness is decreased, thereby reducing the Young's

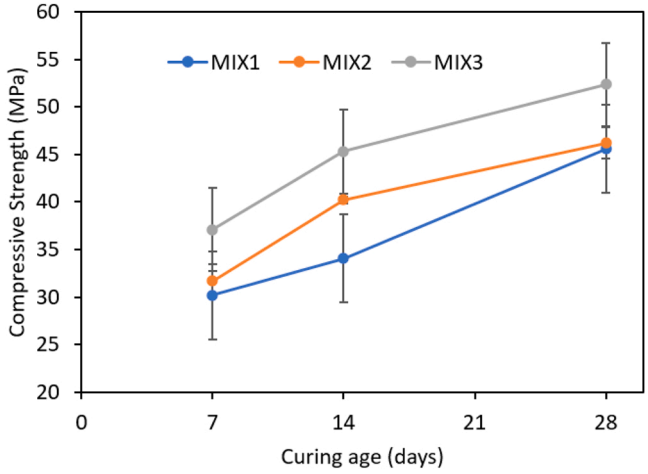

Fig. 3. Average compressive strength of MIX1, MIX2 and MIX3 at different curing ages.

modulus. However, the Young's modulus for all the mixes was observed to be either comparable or lower than that reported in literature for other similar ECCs [9]. As discussed earlier, the reduced matrix densification stemming from high volume of fly ash content must have led to the lower strength and stiffness, as demonstrated in this study.

3.2. *Tensile properties*

The average tensile properties of the three mixes including the first cracking stress, ultimate tensile strength and ultimate strain are summarised in Table 5. MIX1 with the highest fly ash content exhibited the lowest tensile strength of 2.9 MPa. As the fly ash content was lowered

Table 5
Average tensile properties of the base mixes.

Mix ID	First Cracking Stress (MPa)	Tensile Strength (MPa)	Ultimate Tensile Strain (%)
MIX1	2.8	2.9	4.4
MIX2	3.5	3.9	1.7
MIX3	3.6	4.5	3.1

from 1.2 to 1.1 and 1.0 in MIX2 and MIX3 respectively, the tensile strength increased to 3.9 MPa and 4.5 MPa correspondingly. Similar trend was observed for the first cracking stress. In contrast to strength, MIX1 with the highest fly ash volume showed the highest ultimate tensile strain of 4.4 %, whereas MIX2 showed the lowest value. The reduced bonding between the fibre and the matrix in MIX1 would have delayed the pre-mature fibre rupture leading to high ultimate strain capacity [6].

Fig. 4 shows the tensile stress-strain curves for MIX1, MIX2 and MIX3. It can be seen that all the mixes exhibited strain hardening behaviour. A typical fracture surface of a specimen is further displayed in Fig. 5, portraying the fibre bridging and microcracks corresponding to the strain- hardening behaviour observed in Fig. 4.

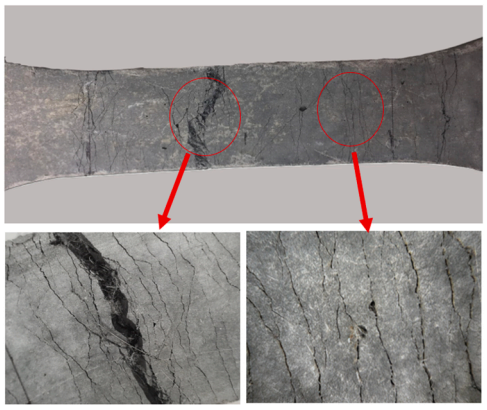

Fig. 5. Microcracks and fibre bridging near the failure surface.

3.3. Microstructural analysis

The morphology of the mixes was observed using SEM and the fibre/matrix interfaces of MIX1 (mix with highest fly ash /silica fume ratio of 1.2:0) and MIX3 (mix with lowest fly ash /silica fume ratio of 1:0.2) are shown in Fig. 6. More voids and unhydrated fly ash were seen in MIX1 than MIX3, whereas more hydrated products and a less porous interface was found in MIX3, explaining its higher strength.

DSC analysis was also conducted for the three mixes to further analyse the hydration compounds present in the matrix based on their decomposition range. In accordance with the SEM images, DSC results revealed a higher formation of hydrates in MIX3 compared to MIX2, and in MIX2 compared to MIX1. As evidenced by the DSC/temperature curves (Fig. 7), at around 116° C, the temperature at which the decomposition of C-S-H and Ettringite occurs and at around 490° C, the temperature at which Portlandite decomposes [33], there was a gradual increase in the area under the curve from MIX1 to MIX3. This trend suggests that the production of hydration products may possibly be higher in MIX3 followed by MIX2 and MIX1.

In general, a pattern of strength increase was observed from MIX1 to MIX2 and from MIX2 to MIX3. This trend can be attributed to the increase in matrix densification arising from the ultra-fine silica fume particles, and the decrease in matrix densification resulting from the spherical fly ash particles in transitioning from MIX1 to MIX2 and from MIX2 to MIX3.

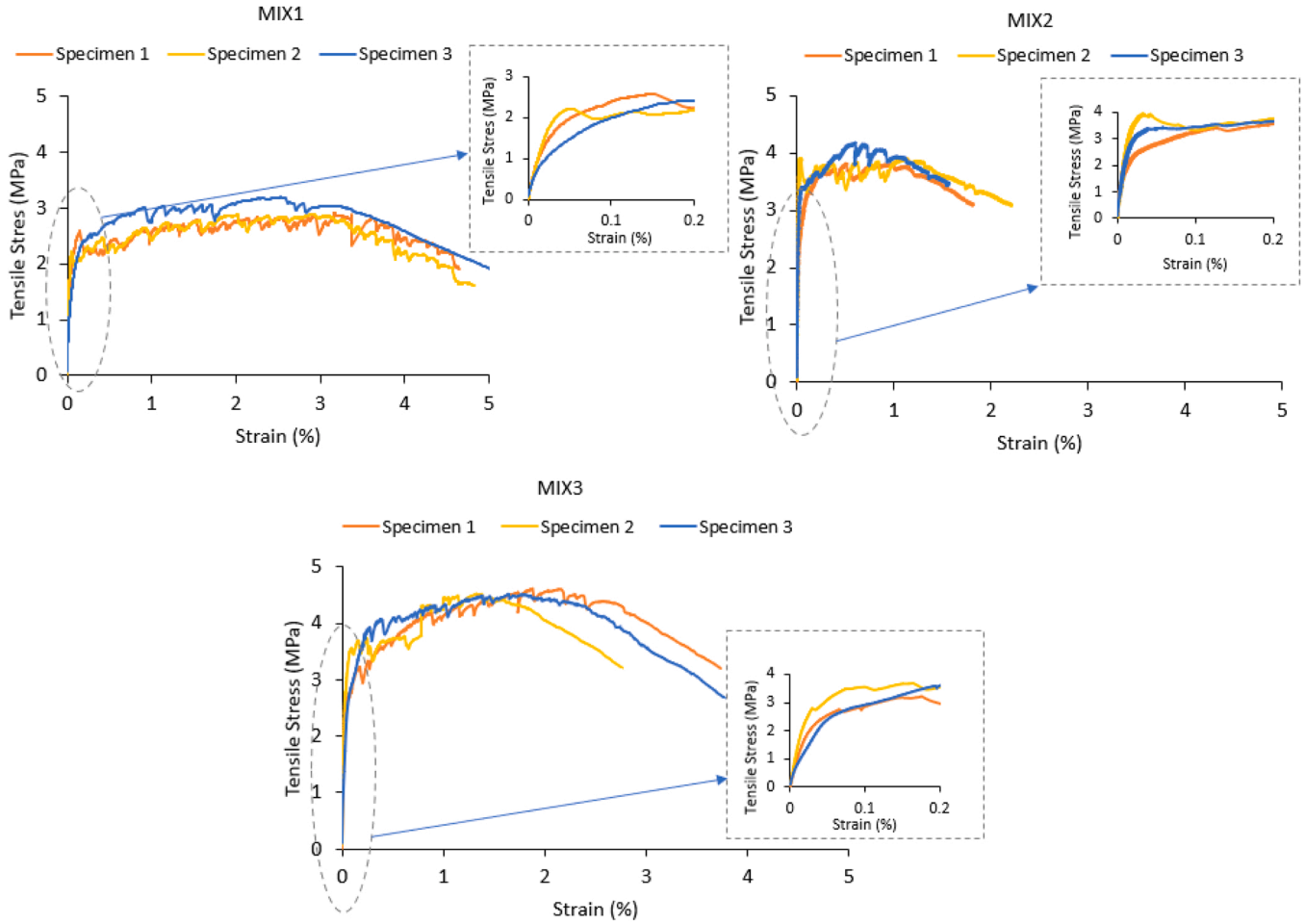

Fig. 4. Tensile stress-strain curves for MIX1, MIX2 and MIX3.

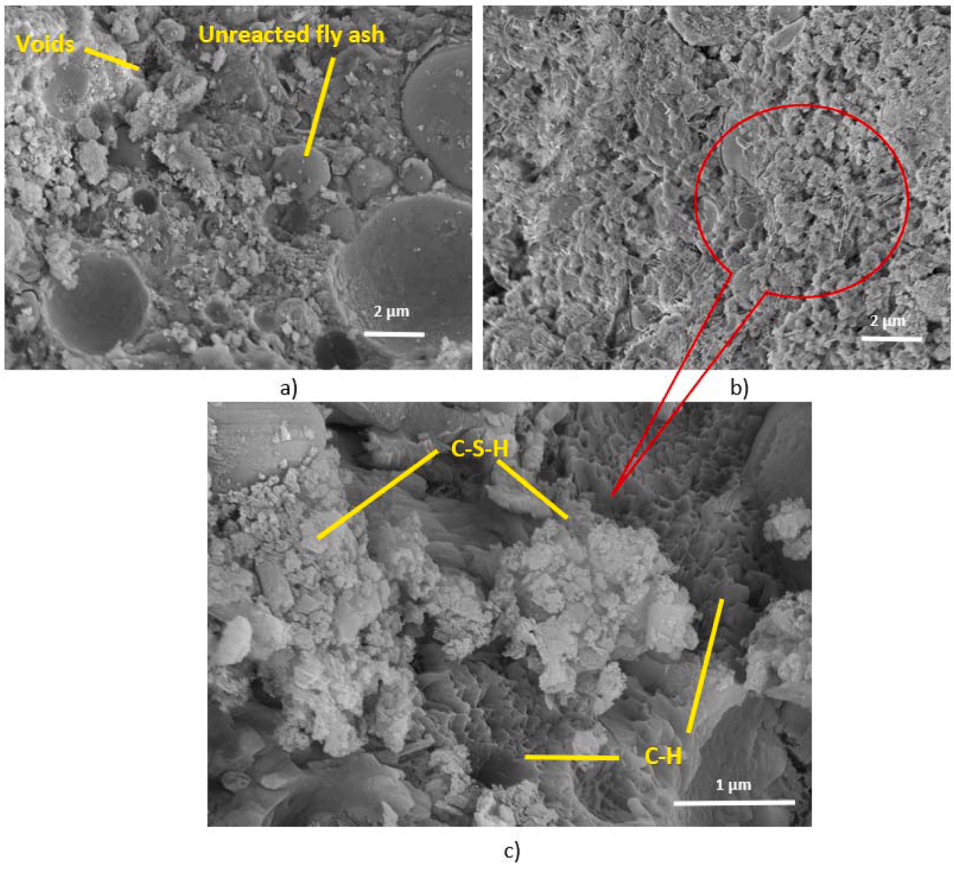

Fig. 6. SEM images of matrices: a) MIX1; b-c) MIX3.

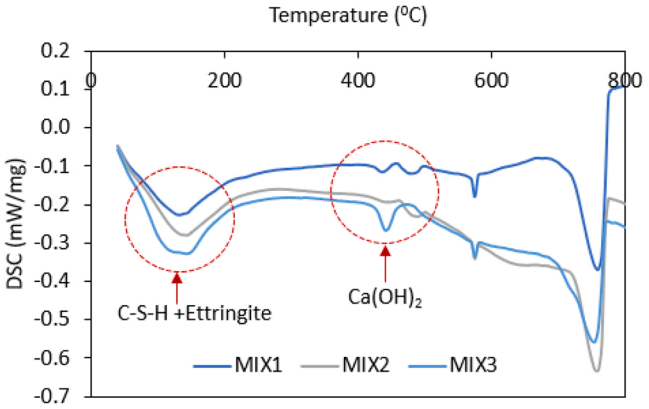

Fig. 7. DSC/Temperature curves for MIX1, MIX2 and MIX3.

As shown in Fig. 6, the large particle size of unreacted or partially reacted fly ash must have increased the porosity of the composite leading to a decrease in the matrix densification. On the other hand, the ultra-fine particles of silica fume must have filled the voids between larger particles and consumed more $Ca(OH)_2$ to form more C-S-H (as confirmed by Fig. 6 and Fig. 7), thereby densifying the interfacial zone. Therefore, MIX1 whose fly ash/silica fume ratio was the highest must have had the weakest fibre/matrix bond contributing to the lowest strength. Similar findings have also been reported in literatures, indicating that incorporating a significant amount of fly ash leads to reduced strength in cement composites [6,34]. However, it should be noted that the mix with the highest fly ash content exhibited the highest ultimate tensile strain. Thus, it can be inferred that the fly ash might have reduced the fibre/matrix interfacial bond and matrix densification, thereby favouring strain. Studies have reported that low matrix densification aids the energy criterion that needs to be satisfied for strain hardening in ECC, and if the interfacial bond between fibre and matrix is strong, the fibres can rupture prematurely when they are pulled out from the matrix [6]. Therefore, the reduced bonding between the fibre and the matrix in MIX1 would have delayed the pre-mature fibre rupture leading to high ultimate strain capacity.

4. Effect of NC on the mechanical properties of ECCs

The effect of NC on the mechanical properties of the PE-Steel-ECCs were investigated by carrying out compressive and tensile tests on the nine NC-ECC mixes with varying NC dosage (0.15 %, 0.2 %, 0.25 %). The results were subsequently compared with those from the base mixes without NC.

4.1. Compressive properties

Fig. 8 displays the average compressive strength of all nine mixes along the three base mixes (MIX1, MIX2, MIX3) without NC. The maximum strength was observed with 0.2 % NC concentration in all the three base mixes. MIX3 with the highest silica fume content and the lowest fly ash content showed the highest strengths for all concentrations of NC as expected. The enhancement in strength in the mixes with NC as compared to the reference mix could be attributed to the strong bonding resulting from NC whilst the reduction in strength at higher dosage of NC could be attributed to fibre agglomeration arising from difficulty of dispersion.

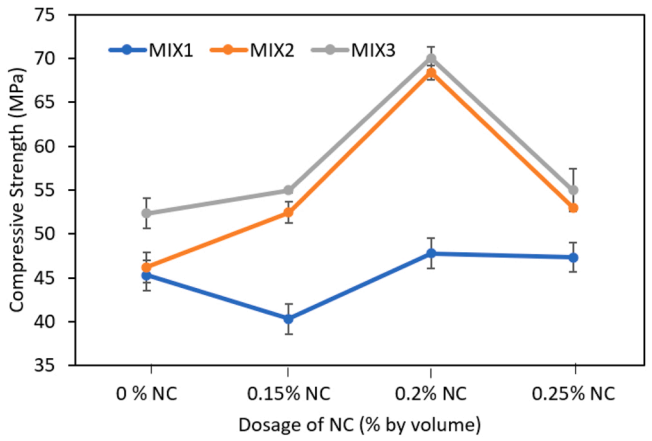

Fig. 8. Effect of NC on average compressive strength of the three base mixes.

4.2. Tensile properties

The average tensile strength and ultimate tensile strains are summarised in Table 6 and the typical tensile stress-strain curves of the six tests for the three base mixes, MIX1 and MIX2 and MIX3 with 0.15 %, 0.2 % and 0.25 % of NC as compared to the reference mix without NC has further been shown in Fig. 9.

It can be observed from Table 6 that the mix with 0.2 % NC gave the maximum tensile strength for all the mixes. For all three sets, mixes with 0.15 % NC resulted in an improvement while mixes with 0.25 % NC showed a slight decrease in tensile strength as compared to the reference mix. When compared among the mixes at the same NC doses, MIX3 with the lowest fly ash content and the highest silica fume content gave the highest strength as expected, while MIX1 with the highest fly ash content and the lowest silica fume content exhibited the lowest strength.

However, the behaviour of tensile strain was not coherent. A negative correlation was expected between strength and strain since matrix densification could potentially limit strain capacity and favour strength. Conversely, the mix with the highest tensile strength (MIX3) did not always correspond to the lowest strain, and the mix with the lowest tensile strength (MIX1) did not always show the highest strain. MIX2 exhibited the lowest strain capacity for all the dosages of NC. Similarly, when comparing strain capacities with NC dosages, MIX3 containing 0.2 % NC showed the highest strain capacity despite being the strongest mix and no consistent pattern was observed between the NC dosages. These irregularities may result from interactions between ingredients. For example, fly ash supports uniform fibre dispersion [35] and this may have reduced fibre agglomeration and favoured strain. In general, all the mixes demonstrated the unique high tensile ductility, and the improvements in tensile strength achieved by adding NC have not compromised the strain compared to the reference mix.

The average crack width and the number of cracks for NC concentration of 0 %, 0.15 %,0.2 % and 0.25 % are further presented in Table 7. The crack widths and number of cracks were calculated after the tensile test using a crack width ruler. Most of the multiple cracks were concentrated within approximately 40 mm interval around failure surface within the gauge length, and this section was chosen for the calculations. For comparison purposes, all the specimens were chosen from a single mix (MIX3). It is evident that the number of cracks is proportional to the tensile strain hardening behaviour. The mix with 0.2 % NC, which exhibited the highest strain capacity, had the greatest number of cracks, while the mix with 0.15 % NC, which demonstrated the lowest strain hardening behaviour, had the fewest cracks. Nevertheless, no coherent pattern was observed in the crack widths.

4.3. Microstructural analysis

The effect of NC could be further examined using SEM images. Figs. 10 and 11 show the SEM images of the fibre/matrix of the mixes with 0 % NC, 0.15 % NC and 0.25 % NC at magnification factors of 10k and 25k respectively. It is evident from these images that the matrix is less porous and denser in the mixes with NC compared to the reference mix and these observations are more prominent in the mix with 0.2 % NC mix.

The reduced porosity in the mixes with NC relative to the reference mix can be attributed to the enhanced degree of hydration (DOH) resulting from the internal curing effect of NC, which arises from the hydrophilic and hygroscopic nature. Moreover, the high aspect ratio and the high specific surface area of NC might also have promoted the strong bonding by availing more hydroxyl groups to hydrogen bond with the cementitious matrix as suggested in previous studies [36]. Consequently, the addition of NC must have enhanced fibre matrix interaction and improved matrix densification, favouring strength compared to the reference mix without NC. In contrast, the reference mixture with 0 % NC showed relatively more unreacted fly ash and increased porosity, making it evident that NC plays an important role in promoting the hydration process and refining the pore structure in the presence of hybrid fibres. These findings are consistent with the performance of NC in NC-cement systems without any fibres as reported in the literature [25,37,38].

On the other hand, when NC was added in excessive quantities, it is likely that the fibres agglomerated making dispersion difficult. Studies have reported that due to the high density of –OH groups present on their surface, cellulose fibrils try to bond with adjacent –OH groups by hydrogen bonds, resulting in fibre agglomeration [39]. This effect is more prominent in nano fibrils due to their larger surface area. Therefore, the decline in strengths in 0.25 % of NC following the maximum strength at 0.2 % can be attributed to fibre agglomeration leading to high porosity and the dosages beyond 0.2 % may be considered excessive. This is also visible from Fig. 11 where the 0.25 % NC mix (Fig. 11d) showed more porous microstructure than 0.2 % and 0.15 % NC mixes (Figs. 11c and 11b). This phenomenon can be further justified using the micrographs obtained through SEM analysis as shown in Fig. 12. As seen from Fig. 12b, when fibres agglomerate, they cannot be readily available at the nano scale for hydration, leading to a less refined pore structure.

This can be further substantiated by the results of DSC analysis. As evidenced in Fig. 13, distinct differences can be observed in the DSC/temperature curves of the NC-ECC mixes with 0.2 % NC compared to their corresponding base mix without NC. Specifically, there is a notable increase in the area under the curves of the mixes with NC as the temperature approaches 116°C, where the decomposition of C-S-H and Ettringite occurs [33]. Additionally, a significant drop in the curves of these mixes is observed between 400° C and 500° C, which can be attributed to decomposition of $Ca(OH)_2$ [40,41]. The simultaneous

Table 6
Average tensile properties of the mixes for different NC dosages.

	MIX1	MIX1-0.15NC	MIX1-0.2NC	MIX1-0.25NC	MIX2	MIX2-0.15NC	MIX2-0.2NC	MIX2-0.25NC	MIX3	MIX3-0.15NC	MIX3-0.2NC	MIX3-0.25NC
Tensile strength (MPa)	2.9	3.1	3.2	2.6	3.9	4.3	4.7	3.5	4.5	5	5.3	4.4
Ultimate tensile strain (%)	4.4	4.1	3.9	3.2	1.7	2.5	2.1	1.9	3.1	2.9	4.1	3.1

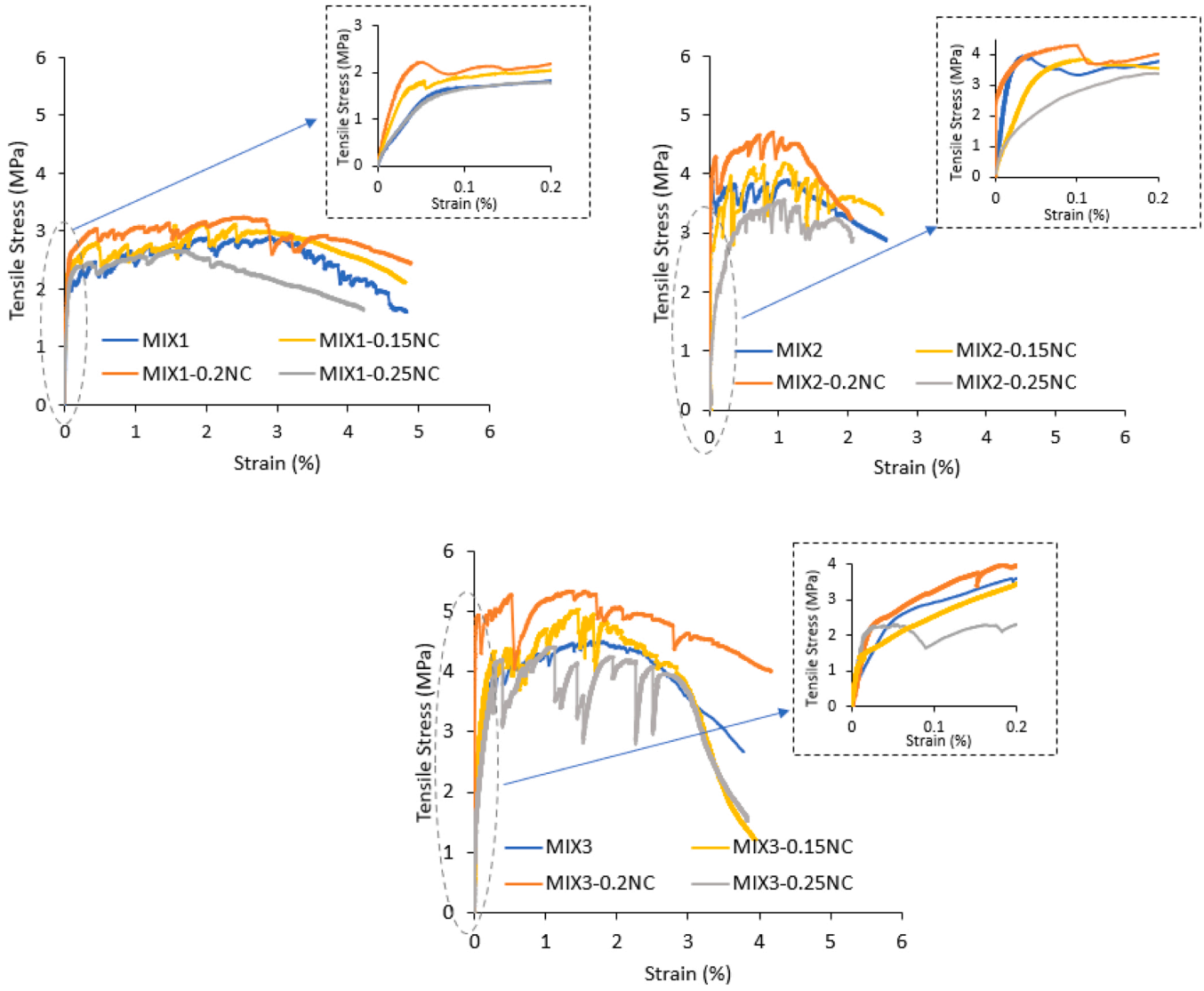

Fig. 9. Typical tensile stress strain curves for all ECC mixes with different NC dosages.

Table 7
Average crack width and number of cracks after tensile failure for different NC dosages.

NC concentration (%)	Average crack width (μm)	Number of cracks (per 40 mm)
0	~56	18
0.15	~57	12
0.2	~62	22
0.25	~54	19

increase in both CSH and $Ca(OH)_2$ peaks can be attributed to the primary hydration reactions producing $Ca(OH)_2$. Although $Ca(OH)_2$ is typically consumed to produce more C-S-H during the hydration process, calcium silicates (such as C_3S and C_2S) can react with water, forming $Ca(OH)_2$. Initially, the formation of $Ca(OH)_2$ from these reactions may have increased the $Ca(OH)_2$ peak in the DSC curve. Similar behaviour was observed in previous studies [42,43]. Hence it can be concluded that more hydration products are formed with addition of NC resulting in higher strength. These findings further confirms that NC promotes the hydration process of hybrid ECC systems, reflecting its role in plane cement systems as reported in literature. [25,37,38].

5. Conclusions

This study developed an innovative and eco-friendly hybrid PE-steel fibre ECC reinforced with nanocellulose (NC), incorporating high-volume fly ash and silica fume. Firstly, three base mixes of the PE-Steel ECCs with varying proportions of fly ash and silica fume were developed and the effect of these mineral admixtures was examined. Thereafter, the base mixes were reinforced with 0.15 % - 0.25 % by weight of NC and the effect of NC on compressive and tensile properties of the HVFA hybrid PE-steel ECC was investigated. Detailed micro-scale analysis was also conducted using SEM and DSC to provide a comprehensive understanding of the experimental results. Based on the obtained results, the following conclusions can be drawn.

- Decreasing the fly ash/silica fume ratio resulted in increased compressive strength, tensile strength, and Young's modulus, but decreased ultimate tensile strain. Specifically, reducing the fly ash ratio from 1.2 to 1.0 increased compressive strength from 46 MPa to 52 MPa, Young's modulus from 14 GPa to 28 GPa, and tensile strength from 2.9 MPa to 4.5 MPa. However, the highest ultimate tensile strain of 4.4 % was observed in the mix with the highest fly ash ratio of 1.2. SEM analysis indicated the presence of unreacted fly

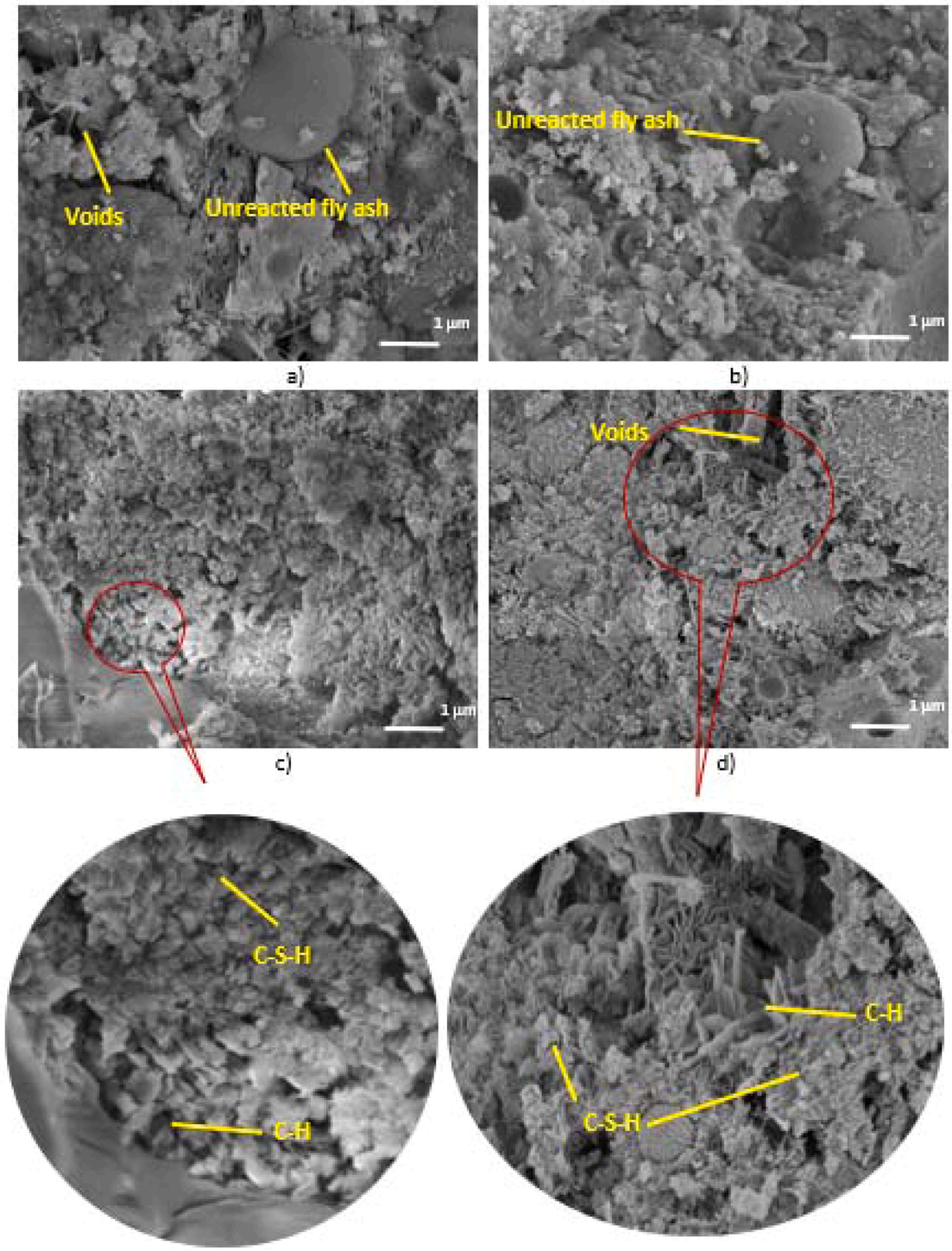

Fig. 10. SEM images of matrix of the mixes: a) 0 % NC; b) 0.15 % NC; c) 0.2 % NC; d) 0.25 % NC (magnification factor-10k).

ash which reduced matrix densification and hence, may have favoured strain.

- The addition of NC up to 0.2 wt% enhanced both compressive and tensile strength compared to the mix without NC (0 % NC) in all the mixes. Any further addition of NC beyond this dosage resulted in a decline in strength. When compared to the reference base mixes, the addition of 0.2 % NC resulted in a 5.5 % improvement in compressive strength for MIX1, a 48 % improvement for MIX2, and a 34 % improvement for MIX3. The corresponding improvements in tensile strength were 10 %, 20 %, and 18 % for MIX1, MIX2, and MIX3, respectively.
- The addition of NC in optimal amounts was crucial for enhancing strength. When used in low quantities, NC did not provide the favourable properties, while excessive amounts led to agglomerations. Additionally, all mixes exhibited typical strain-hardening behaviour, and the matrix densification resulting from NC addition did not negatively impact the strain-hardening properties of the ECC. SEM analysis further confirmed that a denser matrix was achieved with the optimal amount (0.2 wt%) of NC, compared to the more

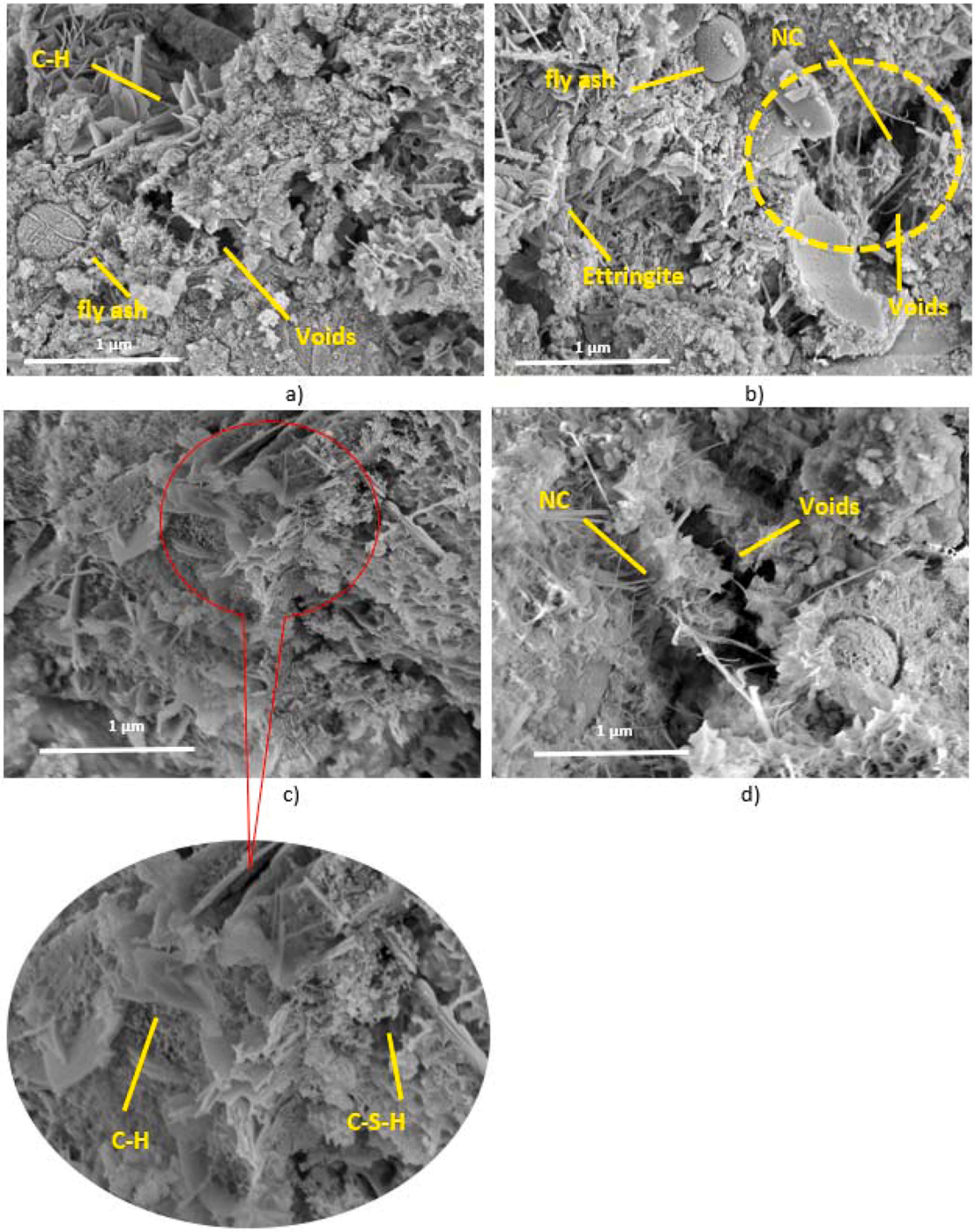

Fig. 11. SEM images of matrix of the mixes: a) 0 % NC; b) 0.15 % NC; c) 0.2 % NC; d) 0.25 % NC (magnification factor-25k).

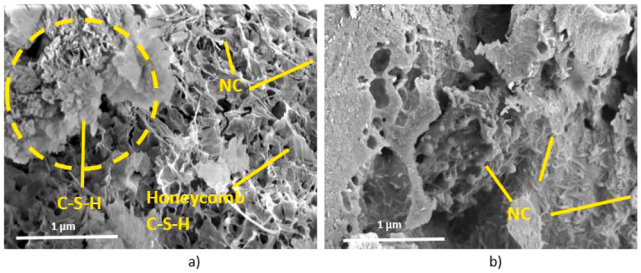

Fig. 12. SEM images: a) NC-ECC with 0.2 % NC; b) NC-ECC with 0.25 % NC.

porous matrix of the mix without NC (0 % NC). However, the NC-ECC with 0.25 % NC showed fibre entanglements and a more porous microstructure than the mix with 0.2 % NC, indicating that NC concentrations above 0.2 wt% are excessive.

- MIX3–0.2NC with fly ash: silica fume ratio of 1.0:0.1 with 0.2 wt% NC concentration gave the best performance with a compressive strength of 70 MPa, ultimate tensile strength of 5.3 MPa and ultimate tensile strain reaching to 4.1 %.

The promising combination of high-performance properties offered by NC suggests that this new material has the potential to outperform existing ECCs. It is anticipated that this novel ECC will serve as a

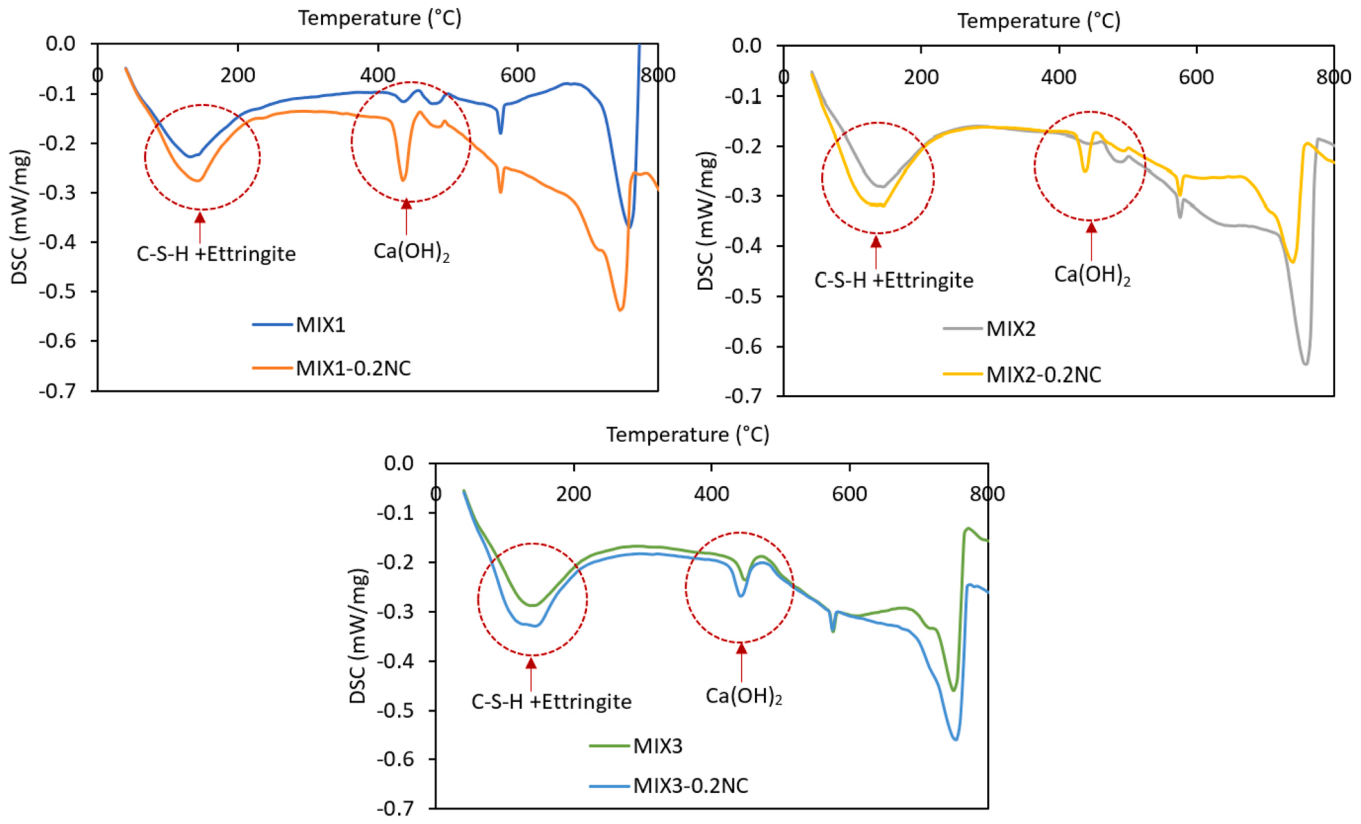

Fig. 13. DSC/Temperature curves for NC-ECC mixes with 0.2 % NC and base mixes with 0 % NC a) MIX1; b) MIX2; c) MIX3.

sustainable material solution with exceptional mechanical properties for use in engineering structures, contributing to reduced environmental impact. Nevertheless, the behaviour of tensile strain with the addition of NC would merit additional investigation, specifically regarding the effect of various proportions of the constituents such as binder material, water-binder ratio, NC, and fibre percentages as a combination on the composite performance. Additionally, micromechanical testing should be conducted to better understand how each parameter influences the strength and energy criteria. Future research could also focus on exploring the interactions between these components and optimizing the mix proportions to enhance the overall performance.

CRediT authorship contribution statement

Sanket Rawat: Writing – review & editing, Validation, Supervision, Methodology, Investigation, Conceptualization. **Daniel Fanna:** Investigation. **Y.X. Zhang:** Writing – review & editing, Supervision, Resources, Project administration, Methodology, Funding acquisition, Conceptualization. **H. Withana:** Writing – original draft, Validation, Methodology, Investigation, Formal analysis, Data curation, Conceptualization.

Declaration of Competing Interest

The authors declare that they have no known competing financial interests or personal relationships that could have appeared to influence the work reported in this paper

Acknowledgment

The authors would also like to acknowledge Dr Laurel George and Dr Richard Wuhrer from the Advanced Materials Characterisation Facility (AMCF), Western Sydney University for access to instrumentation and training.

Data availability

Data will be made available on request.

References

[1] V.C. Li, Engineered cementitious composites (ECC) material, structural, and durability performance, in, in: E. Nawy (Ed.), Concrete Construction Engineering Handbook, CRC Press, 2008, pp. 1–78.
[2] J. Chilvers, et al., Experimental and numerical investigations of hybrid-fibre engineered cementitious composite panels under contact explosions, Eng. Struct. 266 (2022) 114582.
[3] K.T. Soe, Y. Zhang, L. Zhang, Material properties of a new hybrid fibre-reinforced engineered cementitious composite, Constr. Build. Mater. 43 (2013) 399–407.
[4] S. Zhu, Y. Zhang, C. Lee, Polyethylene-steel fibre engineered cementitious composites for bridge link slab application, Structures 32 (2021) 1763–1776.
[5] S.F. Ahmed, M. Maalej, P. Paramasivam, Analytical model for tensile strain hardening and multiple cracking behavior of hybrid fiber-engineered cementitious composites, J. Mater. Civ. Eng. 19 (7) (2007) 527–539.
[6] Wang, S. and V.C. Li, Engineered cementitious composites with high-volume fly ash. 3 (104 Acids Mater. J. , 2007, 233.
[7] R.A. Aldaher, et al., Reducing the Effect of Air Pollution due to Cement Production by Using Low Cement Content Concrete with same or more Efficiency with Normal Concrete, Key Eng. Mater. 895 (2021) 50–58, https://doi.org/10.4028/www.scientific.net/KEM.895.50.
[8] Yang, E.-H., *Designing Added Functions in Engineered Cementitious Composites*. (Doctoral dissertation), The University of Michigan, 2008. ⟨https://hdl.handle.net/2027.42/58406⟩.
[9] Y. Wang, et al., Effect of polyethylene fiber content on physical and mechanical properties of engineered cementitious composites, Constr. Build. Mater. 251 (2020) 118917.
[10] S. Rawat, Y. Zhang, C. Lee, Multi-response optimization of hybrid fibre engineered cementitious composite using Grey-Taguchi method and utility concept, Constr. Build. Mater. 319 (2022) 126040.
[11] Z. Zhang, et al., Matrix design of light weight, high strength, high ductility ECC, Constr. Build. Mater. 210 (2019) 188–197.
[12] Z. Zhang, et al., Sustainable high strength, high ductility engineered cementitious composites (ECC) with substitution of cement by rice husk ash, J. Clean. Prod. 317 (2021) 128379.

[13] Z.S. Metaxa, et al., Nanomaterials in cementitious composites: an update, Molecules 26 (5) (2021) 1430.
[14] A. Hunashyal, et al., Experimental investigation on effect of carbon nanotubes and carbon fibres on the behavior of plain cement mortar composite round bars under direct tension, Int. Sch. Res. Not. 2011 (2011) 1–6.
[15] Ludvig, P., et al. *In-situ synthesis of multiwall carbon nanotubes on Portland cement clinker*. in 11th International Conference on Advanced Materials, *Rio de Janeiro, Brazil*. 20-25 September, 2009.
[16] A.G. Nasibulin, et al., A novel cement-based hybrid material, N. J. Phys. 11 (2) (2009) 023013.
[17] K. Liew, M. Kai, L. Zhang, Carbon nanotube reinforced cementitious composites: an overview, Compos. Part A: Appl. Sci. Manuf. 91 (2016) 301–323.
[18] A. Saloma, I. Imran, M. Abdullah, Experimental investigation on nanomaterial concrete, Int. J. Civ. Environ. Eng. 13 (3) (2013) 15–20.
[19] S.C. Paul, et al., Properties of cement-based composites using nanoparticles: a comprehensive review, Constr. Build. Mater. 189 (2018) 1019–1034.
[20] Pan, Z., et al., *Graphene oxide reinforced cement and concrete*, W.I.P. Organization, Editor. 2013, Google Patents.
[21] S.J. Eichhorn, A. Dufresne, M. Aranguren, Review: current international research into cellulose nanofibres and nanocomposites, J. Mater. Sci. 45 (1) (2010) 1–33, https://doi.org/10.1007/s10853-009-3874-0.
[22] A. Balea, et al., Nanocelluloses: Natural-based materials for fiber-reinforced cement composites. A critical review, p. E518, Polymers 11 (3) (2019), https://doi.org/10.3390/polym11030518.
[23] O.A. Hisseine, et al., Nanocellulose for improved concrete performance: a macro-to-micro investigation for disclosing the effects of cellulose filaments on strength of cement systems, Constr. Build. Mater. 206 (2019) 84–96, https://doi.org/10.1016/j.conbuildmat.2019.02.042.
[24] Z. Rong, et al., Effects of nano-SiO2 particles on the mechanical and microstructural properties of ultra-high performance cementitious composites, Cem. Concr. Compos. 56 (2015) 25–31.
[25] M.I. Haque, et al., A comparative investigation on the effects of nanocellulose from bacteria and plant-based sources for cementitious composites, Cem. Concr. Compos. 125 (2022) 104316.
[26] S. Ahmed, M. Maalej, Tensile strain hardening behaviour of hybrid steel-polyethylene fibre reinforced cementitious composites, Constr. Build. Mater. 23 (1) (2009) 96–106.
[27] L. Brinchi, et al., Production of nanocrystalline cellulose from lignocellulosic biomass: technology and applications, Carbohydr. Polym. 94 (1) (2013) 154–169.
[28] M. Maalej, S.T. Quek, J. Zhang, Behavior of hybrid-fiber engineered cementitious composites subjected to dynamic tensile loading and projectile impact, J. Mater. Civ. Eng. 17 (2) (2005) 143–152.
[29] Withana, H. and Y.S. Zhang, *Behavior of hybrid engineered cementitious composites containing nanocellulose*. Nanotechnology in Construction for Circular Economy, Proceedings of NICOM7, 31 October-02 November, 2022, Melbourne, Australia, 2023: p. 37-41.
[30] M. Khan, Y. Zhang, C. Lee, Mechanical properties of high-strength steel–polyvinyl alcohol hybrid fibre engineered cementitious composites, J. Struct. Integr. Maint. 6 (1) (2021) 47–57.
[31] Standards Australia, Methods of testing concrete. 2014: Sydney, SA. p. 1012-2014.
[32] D. Meng, et al., Mechanical behaviour of a polyvinyl alcohol fibre reinforced engineered cementitious composite (PVA-ECC) using local ingredients, Constr. Build. Mater. 141 (2017) 259–270.
[33] I. Hager, Colour change in heated concrete, Fire Technol. 50 (2014) 945–958.
[34] M. Nili, V. Afroughsabet, The long-term compressive strength and durability properties of silica fume fiber-reinforced concrete, Mater. Sci. Eng.: A 531 (2012) 107–111.
[35] S.F.U. Ahmed, M. Maalej, P. Paramasivam, Flexural responses of hybrid steel–polyethylene fiber reinforced cement composites containing high volume fly ash, Constr. Build. Mater. 21 (5) (2007) 1088–1097.
[36] Y. Cao, et al., The influence of cellulose nanocrystal additions on the performance of cement paste, Cem. Concr. Compos. 56 (2015) 73–83.
[37] O.A. Hisseine, A.F. Omran, A. Tagnit-Hamou, Influence of cellulose filaments on cement paste and concrete, J. Mater. Civ. Eng. 30 (6) (2018) 04018109, https://doi.org/10.1061/(asce)mt.1943-5533.0002287.
[38] O. Onuaguluchi, D.K. Panesar, M. Sain, Properties of nanofibre reinforced cement composites, Constr. Build. Mater. 63 (2014) 119–124, https://doi.org/10.1016/j.conbuildmat.2014.04.072.
[39] B. Wang, M. Sain, Isolation of nanofibers from soybean source and their reinforcing capability on synthetic polymers, Compos. Sci. Technol. 67 (11-12) (2007) 2521–2527.
[40] L. Jiao, et al., Natural cellulose nanofibers as sustainable enhancers in construction cement, PLoS One 11 (12) (2016) e0168422.
[41] H. Haddad Kolour, W. Ashraf, E.N. Landis, Hydration and early age properties of cement pastes modified with cellulose nanofibrils, Transp. Res. Rec. 2675 (9) (2021) 38–46.
[42] K. Hassannezhad, et al., Effect of metakaolin and lime on strength development of blended cement paste, Constr. Mater. 2 (4) (2022) 297–313.
[43] Y. Feng, et al., Hydration and strength development in blended cement with ultrafine granulated copper slag, PLoS One 14 (4) (2019) e0215677.